ORIGINAL ARTICLE

Clonal dynamics of circulating tumor DNA during immune checkpoint blockade therapy for melanoma

Erina Takai[1,2] | Wataru Omata[2,3] | Yasushi Totoki[2] | Hiromi Nakamura[2] |
Satoshi Shiba[2] (iD) | Akira Takahashi[3] | Kenjiro Namikawa[3] (iD) | Taisuke Mori[4] |
Naoya Yamazaki[3] (iD) | Tatsuhiro Shibata[2,5] (iD) | Shinichi Yachida[1,6,7] (iD)

[1]Department of Cancer Genome Informatics, Graduate School of Medicine, Osaka University, Osaka, Japan

[2]Division of Cancer Genomics, National Cancer Center Research Institute, Tokyo, Japan

[3]Department of Dermatologic Oncology, National Cancer Center Hospital, Tokyo, Japan

[4]Department of Diagnostic Pathology, National Cancer Canter Hospital, Tokyo, Japan

[5]Laboratory of Molecular Medicine, The Institute of Medical Sciences, The University of Tokyo, Tokyo, Japan

[6]Integrated Frontier Research for Medical Science Division, Institute for Open and Transdisciplinary Research Initiatives (OTRI), Osaka University, Osaka, Japan

[7]Division of Genomic Medicine, National Cancer Center Research Institute, Tokyo, Japan

Correspondence
Tatsuhiro Shibata, Division of Cancer Genomics, National Cancer Center Research Institute, 5-1-1 Tsukiji, Chuo-ku, Tokyo 1040045, Japan.
Email: tshibata@ncc.go.jp

Shinichi Yachida, Department of Cancer Genome Informatics, Graduate School of Medicine, Osaka University, 2-2 Yamadaoka, Suita, Osaka 5650871, Japan.
Email: syachida@cgi.med.osaka-u.ac.jp

Abstract

Assessment of treatment efficacy of immune checkpoint inhibitors in melanoma patients is difficult as the response to these therapies varies among patients or lesions. The clonal evolution of cancer during immune checkpoint blockade therapy could cause treatment resistance. We investigated the potential of liquid biopsy in monitoring the mutational profiles of metastatic melanoma during immunotherapy. Plasma samples collected from 21 Japanese metastatic melanoma patients before immune checkpoint blockade therapy were subjected to whole-exome sequencing (WES). Furthermore, 14 Japanese patients with melanoma were enrolled for longitudinal analysis of circulating tumor DNA (ctDNA). Plasma samples were collected prospectively before and during therapy and sequenced. WES of the pretreatment plasma from Japanese melanoma patients showed detectable ctDNA levels with wide ranges of variant allele frequencies within a sample, suggesting clonal and subclonal mutations in ctDNA. In targeted sequencing using longitudinal samples, ctDNA levels correlated with increased tumor size, while ctDNA content immediately decreased after a surge in a patient exhibiting pseudo-progression, suggesting the potential of ctDNA analysis in discriminating between pseudo- and true progression. Mutant ctDNA levels showed different patterns within the clinical course of specific patients, suggesting that these mutations were derived from different tumor clones with distinct

---

Abbreviations: ctDNA, circulating tumor DNA; LDH, lactate dehydrogenase; PD, progressive disease; PR, partial response; SD, stable disease; SNVs, single nucleotide variations; VAF, variant allelic frequency; WES, whole-exome sequencing.

Erina Takai and Wataru Omata contributed equally to this study.

------

therapeutic responses. During further investigation, WES of plasma samples from 1 patient showed marked differences in the mutational profiles of ctDNA, including expansive tumor evolution during an acute exacerbation. Immunotherapy may induce characteristic clonal evolutions of tumors; longitudinal analysis of ctDNA has the potential of determining these tumor evolution patterns and therapeutic responses.

KEYWORDS

circulating tumor DNA, clonal evolution, immune checkpoint inhibitor, liquid biopsy, melanoma

1 | INTRODUCTION

Immune checkpoint inhibitors, including anti-PD-1 and anti-CTLA-4 antibodies, have shown promise in treating various cancers.[1-8] However, the efficacy and response to immunotherapy vary among tumor sites in patients, with only a subset of patients responding to these therapies, making it difficult to determine the treatment efficacy of immunotherapy compared with conventional chemotherapy. Patients who initially respond to therapy may exhibit cancer progression during the course of treatment. Cancer cell clones evolve dynamically, and changes in their composition cause acquired resistance to molecular targeted therapies.[9,10] Riaz et al[11] used biopsy specimens to investigate changes in the mutational profile of melanomas and tumor immune microenvironments during nivolumab therapy. Tumor samples obtained before and after (23-29 d) initiation of therapy were assessed using WES, transcriptomics, and T cell receptor sequencing. Clonal evolution of cancer, including putative selection due to immunotherapy, is observed during treatment. A similar study demonstrated dynamic changes in the mutation-associated neoantigen landscape upon administering immune checkpoint blockade therapies and analyzed paired pretreatment and resistant tumors obtained from non–small-cell lung cancer patients.[12] However, the longitudinal clonal evolution of melanoma cells subjected to immune checkpoint therapy remains unclear. This can be attributed to the difficulty in repetitively sampling tumor tissues and collecting sufficient cancer tissues from different sites in a metastatic patient.

Analysis of circulating tumor DNA (ctDNA), a major target of liquid biopsy, enables researchers to determine mutational changes in cancer cells' genome without the need for invasive tissue biopsy. ctDNA harbors mutations arising from multiple cancer clones from different sites of the tumor. Changes in ctDNA (mutations in *BRAF* and *NRAS*) in patients with melanoma correlate with response to treatment.[13-17] Clonal changes, such as acquired resistance to targeted therapies, have been analyzed using ctDNA analysis.[18,19]

Malignant melanoma is extremely rare in Japan, and acral and mucosal subtypes are common. In this study, we performed WES using plasma DNA from 21 Japanese patients with malignant melanoma before being treated with immune checkpoint inhibitors. Moreover, we performed targeted deep sequencing of plasma DNA extracted from another cohort of 14 Japanese patients with melanoma and assessed mutational changes during immune checkpoint blockade therapies.

2 | PATIENTS AND METHODS

2.1 | Ethics statement

The experimental protocols were approved by the institutional review board at the National Cancer Center (approval number 2014-327). Written informed consent was obtained from all patients. The methods were carried out in accordance with the approved guidelines (The Ethical Guidelines for Medical and Health Research Involving Human Subjects and The Ethical Guidelines for Human Genome/Gene Analysis Research).

2.2 | Patients and samples

The study involved patients with malignant melanoma treated at the National Cancer Center Hospital, Tokyo, Japan. Patients were staged using the classification of the American Joint Committee on Cancer, 8th edition. Plasma samples were collected before and during treatment.

2.3 | Blood processing and plasma DNA extraction

For retrospective WES analysis of plasma DNA, plasma samples were obtained from the National Cancer Center Biobank with approval from the National Cancer Center Biobank management committee. Peripheral venous blood samples were centrifuged in EDTA-containing tubes at 1600 *g* for 10 min at 4°C to isolate plasma, which was stored at −80°C until further use. For longitudinal analysis of plasma DNA, blood was centrifuged in EDTA-containing tubes at 1300 *g* for 10 min at 4°C. Separated plasma was aliquoted and stored at −80°C within 2 h of blood collection.

Before DNA extraction, plasma samples were centrifuged at 16 000 *g* for 10 min at 4°C to remove cell debris. Circulating DNA

was extracted from 2 to 5 mL of plasma using the QIAamp DNA Circulating Nucleic Acid Kit (QIAGEN) in accordance with the manufacturer's instructions, eluted in 60 µL of elution buffer, and stored at 4°C. Eluted plasma DNA was quantified using SYBR Green I real-time polymerase chain reaction (PCR) and human LINE-1 sequences.[20] PCR was performed in a 20-µL reaction volume, containing 3 µL extracted plasma DNA, 0.5 µM each of the forward (5′-TCACTCAAAGCCGCTCAACTAC-3′) and reverse primers (5′-TCTGCCTTCATTTCGTTATGTACC-3′), and 1× iTaq SYBR Green Supermix (Bio-Rad). PCR was performed with the following thermal cycling conditions: 2 min at 94°C and 35 cycles of 10 s at 94°C, 15 s at 58°C, and 15 s at 70°C. A standard calibration curve was plotted using 4-fold serial dilutions of human genomic DNA (Promega) up to a 8 ng/reaction. Each sample was assayed in triplicate.

2.4 | Genomic DNA extraction

Genomic DNA was extracted from tissue samples using the QIAamp DNA Mini Kit (for frozen tissue samples, QIAGEN) or QIAamp DNA FFPE Tissue Kit (for FFPE samples, QIAGEN) in accordance with the manufacturer's instructions. Eluted genomic DNA was processed using the Covaris Ultrasonicator (Covaris) before preparing the sequencing library.

2.5 | WES

Whole-exome sequencing libraries were prepared from plasma DNA samples and germline DNA samples using the combination of KAPA Hyper Prep Kit (KAPA Biosystems) and SureSelect Target Enrichment System (Agilent Technologies) as described previously.[21] Briefly, 7.7-100 ng of input DNA were subjected to end repair, A-tailing, and ligated to the Agilent SureSelect adapter. After (solid-phase reversible immobilization) cleanup, the adapter-ligated DNA was amplified using PCR (6-9 cycles). Target capture and library preparation were performed using the Agilent SureSelect Human All Exon Kit V5 in accordance with the manufacturer's instructions. Sequencing was performed using the Illumina HiSeq2500 system (Illumina).

2.6 | Targeted sequencing

Plasma DNA samples, genomic DNA obtained from germline DNA samples from peripheral blood leukocytes, and tumor DNA samples were subjected to targeted capture sequencing. Sequence library preparation, target capture, and WES were performed using the KAPA Hyper Prep Kit (Kapa Biosystems) and SureSelect Target Enrichment System (Agilent Technologies). The whole exons of 74 genes (Table S1) were subjected to targeted deep sequencing using a custom panel. Among the 74 genes, 33 were selected based on the above WES data and are concretely mutated genes listed in COSMIC Cancer Gene Census (https://cancer.sanger.ac.uk/census). Two

genes were added as they were reported as significantly mutated genes in melanoma in a previous report,[22] even though they were not detected by our WES. Other genes were chosen based on their relationships to the response of immune check point inhibitors[23,24] or BRAF inhibitors,[25] or based on the clinical actionability of molecular targets[26] (Table S1). Sequencing was performed using the Illumina HiSeq2500 system (Illumina).

2.7 | Detecting somatic mutations in plasma DNA

Paired-end reads were aligned to the human reference genome (GRCh37) using the Burrows-Wheeler Aligner[27] for the plasma DNA and matched germline DNA samples. Probable PCR duplications, for which paired-end reads aligned to the same genomic position, were removed, and pileup files were generated using SAMtools[28] and an in-house developed program. The following cut-off values were used for base selection to identify the somatic point mutations (single nucleotide variations [SNVs] and short indels): mapping quality score of at least 20 and base quality score of at least 10. For WES, inactivating mutations and hotspot mutations with at least 10 COSMIC hotspot mutations were selected using the following filtering conditions: (a) the numbers of reads supporting a mutation for plasma DNA were at least 4 with a variant allelic frequency of plasma DNA (TVAF) ≥ 0.004; (b) TVAF of matched germline DNA was < 0.03 and 0.01 for TVAF ≥ 0.15 and 0.15 > TVAF ≥ 0.004, respectively. Other somatic mutations were selected using the following filtering conditions: (a) the numbers of reads supporting a mutation for plasma DNA were at least 4 and 7 with a variant allelic frequency of plasma DNA (TVAF) ≥ 0.15 and 0.15 > TVAF ≥ 0.02, respectively; (b) TVAF of matched germline DNA was < 0.03 and 0.01 for TVAF ≥ 0.15 and 0.15 > TVAF ≥ 0.02, respectively. For targeted deep sequencing, the following filtering conditions were used: (a) the numbers of reads supporting a mutation for plasma DNA were at least 8 and 12 for SNVs and indels, respectively; (b) TVAF of matched germline DNA < 0.03. Due to the sequence-specific nature of sequencing errors, the read information from all germline DNA samples was grouped to reliably discriminate between true and false positives. Subsequently, we used the following filters: (a) the ratio of variant allele frequency of grouped germline DNA (NVAF) and plasma DNA (TVAF), NVAF/TVAF < 0.05; (b) all samples with more than 2 somatic mutations (SNV and/or indel) within any 10 bp window and TVAF < 0.2 were discarded; and (c) mutations must be recognized by the forward and reverse reads of > 5% of all supported reads. Additionally, the following filters were applied for WES: (a) NVAF must be less than 0.004 and 0.006 for SNVs and indels, respectively; (b) P-value of Fisher exact test for the numbers of supported and non-supported reads of a mutation in plasma DNA and grouped germline DNA must be < 0.0001. For targeted deep sequencing, mutations with a root mean square mapping quality score < 40 for reads covering the mutation were discarded. For somatic mutations in the plasma DNA, some mutations were also found in paired normal peripheral lymphocyte DNA at low frequencies. Such mutations were considered

somatic mutations in normal lymphocytes associated with clonal hematopoiesis and excluded from ctDNA analysis. ctDNA levels, expressed in human genome equivalents per mL of plasma, were calculated by multiplying the cell-free circulating DNA level based on the percentage of mutant allele fraction measured using sequencing.

3 | RESULTS

Immune checkpoint blockade is usually applicable for patients with advanced and metastatic melanoma. As ctDNA contains tumor DNA from different lesions in a patient, sequence analysis of plasma DNA has the potential to detect mutations in a heterogeneous population of tumor cells. We conducted a retrospective WES analysis of plasma DNA using a cohort of 21 patients with metastatic melanoma

treated with nivolumab to determine their ctDNA mutational profiles (Table S2).

The median unique sequence coverage was 439× (range 349-583×). We detected somatic mutations in the ctDNA from all samples (4-163 per sample; Figure 1A and Table S3). Cancer-related genes, such as *BRAF* (n = 4), *GNAS* (n = 3), and *GRIN2A*, *NF1*, *PTEN*, and *TP53* (n = 2 each), were frequently mutated (Figure 1A), indicating that ctDNA is detectable in patients before treatment.

We then evaluated the VAF of somatic mutations detected in plasma DNA. VAF for each sample was 0.026-0.371 (median 0.039; Figure 1B). Therefore, plasma DNA sequencing analysis identified clonal and subclonal mutations or simultaneous amplification of mutant genes.

To investigate longitudinal changes in ctDNA from patients subjected to immune checkpoint blockade therapy, we prospectively
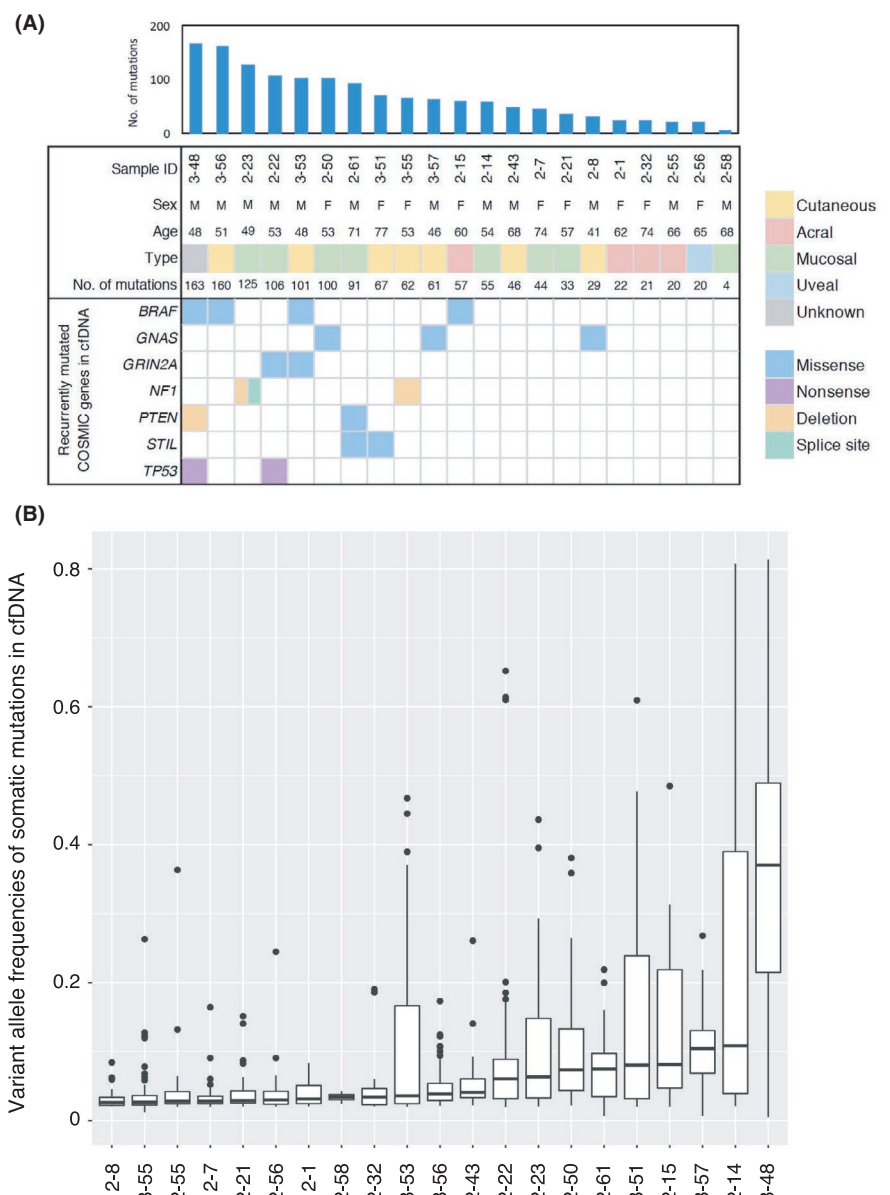

FIGURE 1 Whole-exome sequencing (WES) of plasma DNA from Japanese patients with metastatic melanoma. A, The top bar plot shows the number of somatic mutations identified in each sample. The recurrently mutated genes listed in the COSMIC Cancer Gene Census are shown in the left-most column. B, Variant allele frequencies of somatic mutations detected in plasma DNA. Box plots indicating the variant allele frequencies of mutations detected in each sample. Each box shows the median (central line), inter-quartile range (box), and ±1.5 × inter-quartile range (whiskers)

TABLE 1 Characteristics of patients subjected to targeted sequencing analysis

Case#	Sex	Age	Number of cfDNA samples	Sampling periods (d)	Type	Location of primary tumor	Stage	Treatment	Overall response	Tumor sample
4	F	42	10	342	Cutaneous	Back	IV	Surgery, anti-PD-1	SD	Not available
5	M	74	9	334	Uveal	Choroid	IV	Anti-PD-1	SD	Available
8	M	73	13	301	Uveal	Choroid	IV	Radiation, anti-PD-1	SD	Not available
9	M	56	4	110	Acral	First toe	IV	Anti-CTLA-4, anti-PD-1	SD	Available
11	M	39	2	78	Cutaneous	Knee	IV	Anti-CTLA-4	SD	Not available
12	M	68	7	111	Mucosal	Nasal cavity	IV	Anti-CTLA-4, anti-PD-1	PD	Not available
16	F	69	8	236	Mucosal	Urethral	IV	Anti-CTLA-4, anti-PD-1	PR	Not available
17	M	85	11	253	Acral	Sole	IV	Surgery, anti-PD-1	SD	Available
18	M	66	10	253	Uveal	Choroid	IV	Anti-PD-1	PR	Not available
23	F	77	6	191	Cutaneous	Femur	III	Anti-CTLA-4	PR	Available
25	M	71	2	61	Mucosal	Esophagus	IV	Anti-PD-1	PD	Not available
29	F	64	7	212	Cutaneous	Head	IV	Surgery, anti-PD-1	PR	Not available
38	M	44	4	133	Acral	Sole	IV	Anti-CTLA-4	SD	Available
39	M	62	3	113	Mucosal	Nasal cavity	IV	Anti-PD-1	PR	Not available

Abbreviations: cfDNA, cell-free DNA; PD, progressive disease; PR, partial response; SD, stable disease.

collected plasma samples from melanoma patients to be administered nivolumab or ipilimumab. Among the 19 melanoma patients who were excluded from WES and were prospectively enrolled, plasma samples were available pre- and post-initiation of therapy for 14 cases, including cutaneous (n = 4), mucosal (n = 4), acral (n = 3), and uveal (n = 3) melanomas (Table 1). We collected 2-13 plasma samples/patient (median 7) before and during treatment (range 61-342 d). In cases 4, 17, and 29, immunotherapy was initiated after surgery. Radiotherapy was performed in case 8 before anti-PD-1 therapy. In case 9, the BRAF/MEK inhibitor, vemurafenib, was administered before the immune checkpoint blockade therapy. Quantitative PCR showed time-dependent dynamic changes in DNA content in the plasma for cases 5, 9, 17, 23, and 38 (Figure S1 and Table S4).

To accurately detect somatic mutations in low abundance ctDNA in plasma using deep sequencing, we designed a gene panel, including mutated genes from our WES data, previously identified mutated genes in melanoma, genes related to response to immune check point inhibitors[23,24] or BRAF inhibitors,[25] and clinical actionable driver genes associated with potential targeted therapies.[26] Table S1 lists the exons of 74 genes targeted.

Targeted deep sequencing of the extracted plasma DNA had a median unique sequence coverage of 2021× (range 1139-3005×, Table S4). We detected somatic mutations in ctDNA with a threshold of VAF > 0.006. Subsequently, we monitored the changes in the amounts of mutant DNA during treatment (Table S5). We considered identical mutations detected at different time points in the same patient to be true mutations, although with low VAF, and included mutations with 0.003 < VAF < 0.006.

We identified changes in the repeatedly detected, identical mutant ctDNA in cases 4, 8, 9, 12, 16, 17, 18, and 39 (Figure 2). As the total amount of plasma DNA changed over time, we determined the amounts of mutant DNA by multiplying the level of plasma DNA with the percentage of mutant alleles measured using sequencing.

The changes in ctDNA levels were correlated with the patients' clinical response and serum concentrations of lactate dehydrogenase (LDH) as a clinical biomarker for melanoma. The amounts of ctDNA decreased during the PR in cases 12, 18, and 39. Mutant ctDNA was undetectable during PR in cases 12 and 18 (Figure 2D,G). Conversely, the amounts of ctDNA increased during PD in cases 4, 9, 12, and 16 (Figure 2A,C-E).

Transient increases in ctDNA after the initiation of treatment were observed in cases 8 and 18. In case 18, ctDNA levels were transiently elevated at week 15 and then maintained at a very low or undetectable level during follow-up. At 9 wk after the initiation of nivolumab, computed tomography showed pseudo-progression based on the increase in a target lesion size. Subsequently, liver metastasis gradually slowed and resulted in PR at week 63 (Figure 2G).

Some cases showed different patterns of changes in mutant ctDNA levels, even in the same patient. In case 4, a mutation in *MLL3* (the only mutation detected before surgery for cutaneous melanoma on the back) disappeared after resection (Figure 2A). Although mutant *MLL3* was undetectable at the time of appearance of brain metastasis (11 wk), the amount of ctDNA with mutant *MLH1* increased until the initiation of nivolumab treatment. Subsequently, the levels of both mutations elevated during PD, suggesting different mutational profiles in the different lesions, such as primary and metastatic tumors (Figure 2A). Case 8 was administered nivolumab after radiotherapy for bone metastases, and SD was monitored at weeks 9, 22, and 33. Two *MSH3* mutations were detected in the plasma throughout the observation period. However, mutations in *ARID1B* transiently increased during and 3 mo after irradiation, indicating the differential nature of acquiring *MSH3* and *ARID1B* mutations (Figure 2B). Therefore, ctDNA analysis has the potential to detect

---

FIGURE 2 Longitudinal changes in mutant circulating tumor DNA (ctDNA) in immunotherapy-treated melanoma patients. A, The amounts of mutant DNA and lactate dehydrogenase (LDH) in plasma are shown on the left, and magnetic resonance images are shown on the right for case 4. The red arrowheads and circles indicate the tumor location. In case 4, brain metastasis was observed 3 mo after surgery, and nivolumab therapy was initiated following radiation therapy. Evaluation at week 11 showed radiographic response accompanying undetectable ctDNA. Mutant ctDNA levels increased during disease progression with new brain metastasis. B, Case 8 was treated with nivolumab following radiotherapy for bone metastases, and the disease was stable at weeks 9, 22, and 33. Two mutations were highly elevated during radiotherapy and 17 wk after the initiation of nivolumab. C, Case 9 underwent 4 cycles of ipilimumab. Radiographic progression with the spread of subcutaneous tumor was documented at week 13. Therapy was discontinued due to immune-related adverse effects. Increased levels of ctDNA were observed at week 14. D, Case 12 had subcutaneous, hepatic portal lymph node, adrenal gland (red arrowhead), and peritoneal metastases at the beginning of immunotherapy. After treatment with ipilimumab for 2 cycles, we initiated nivolumab therapy. Although the radiographic response was noted at week 9 as the adrenal gland metastasis decreased, peritoneal metastases progressed at week 14. While ctDNA decreased to undetectable levels at week 9, multiple mutant ctDNAs were detected at weeks 14 and 16. E, Case 16 was treated with nivolumab after discontinuation of ipilimumab. Mutant ctDNA levels were elevated at the beginning of nivolumab treatment, with increases in lung metastasis. ctDNA levels were increased after a temporary decrease in week 13. Imaging showed a new brain metastasis at week 24. F, In case 17, after surgery for inguinal lymph node metastasis, the residual tumor was treated with nivolumab for 4 cycles, and therapy was discontinued due to immune-related adverse effects. However, computed tomography showed an SD. ctDNA and inguinal lymph node metastasis were consistently observed during follow-up. G, In case 18, pseudo-progression was noted as liver metastasis slightly increased 9 wk after initiation of nivolumab therapy. Thereafter, the lesion gradually decreased and indicated a PR at week 63. While transient elevation of ctDNA was observed at week 15, it rapidly decreased at week 18. H, Case 39 was suspected of having new metastasis in the sternal lymph node 9 wk after initiation of nivolumab therapy. This patient underwent radiotherapy for sternal lymph node in addition to nivolumab, which resulted in PR at week 19. hGE, human genome equivalent; Ipi, ipilimumab; Nivo, nivolumab; PD, progressive disease; PR, partial response; RT, radiation therapy; SD, stable disease

(A) Case 4

(B) Case 8

(C) Case 9

(D) Case 12

(E) Case 16

(F) Case 17

(G) Case 18

(H) Case 39
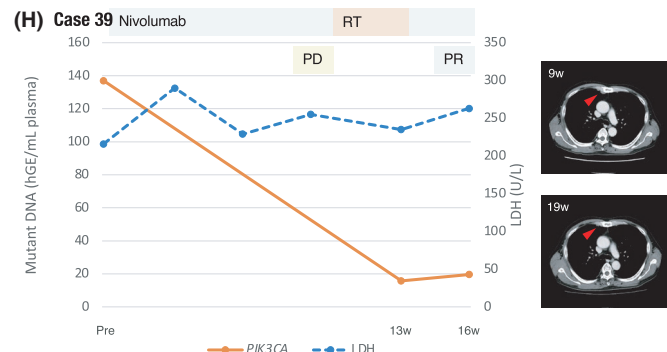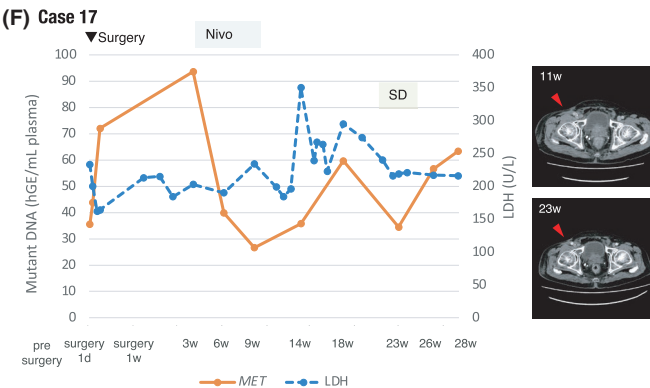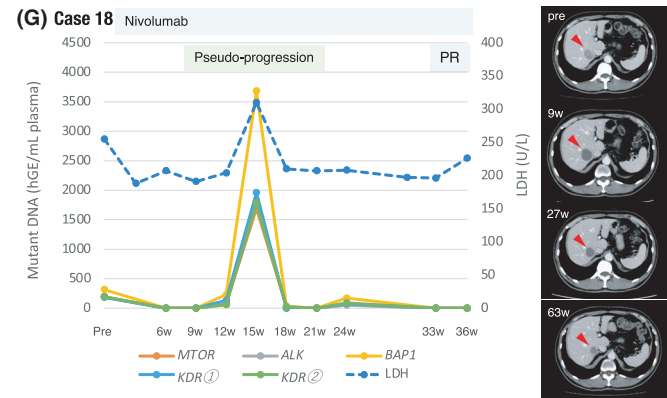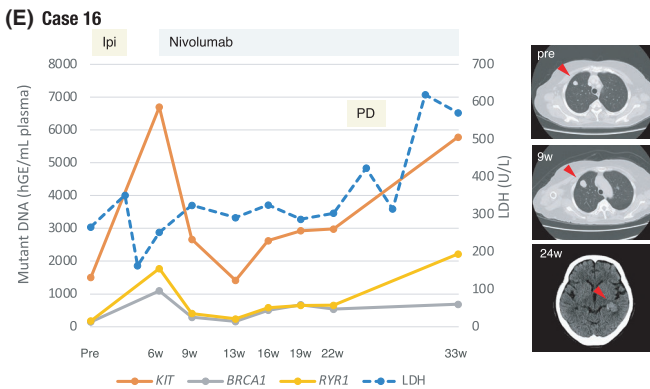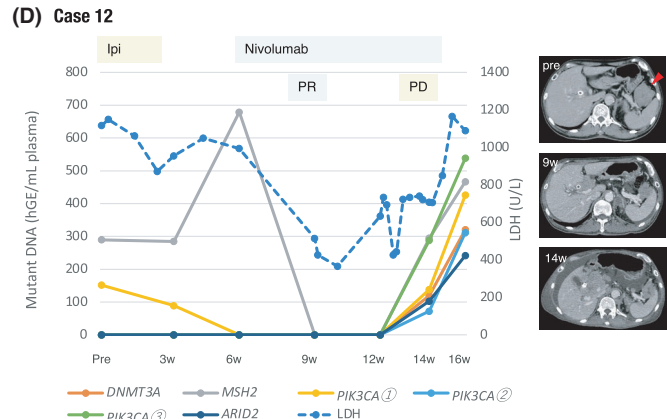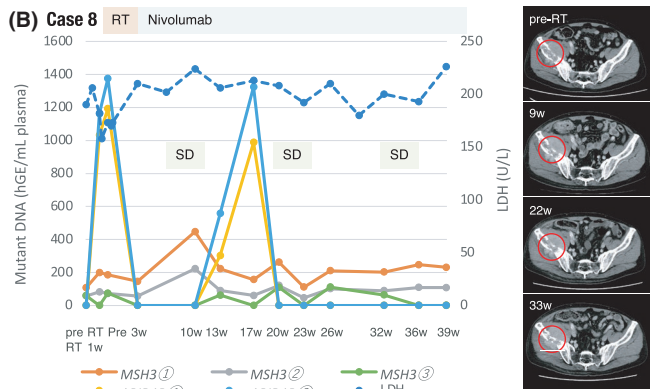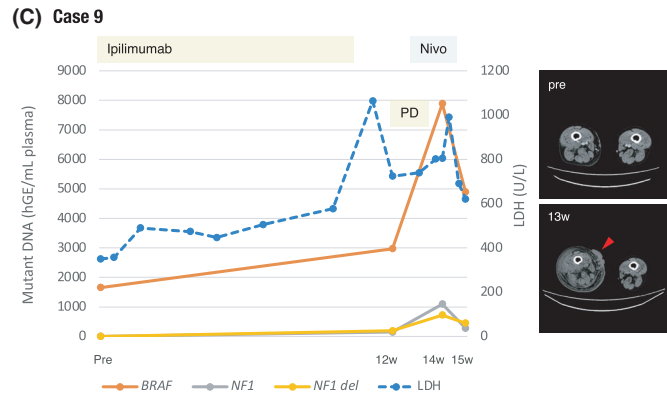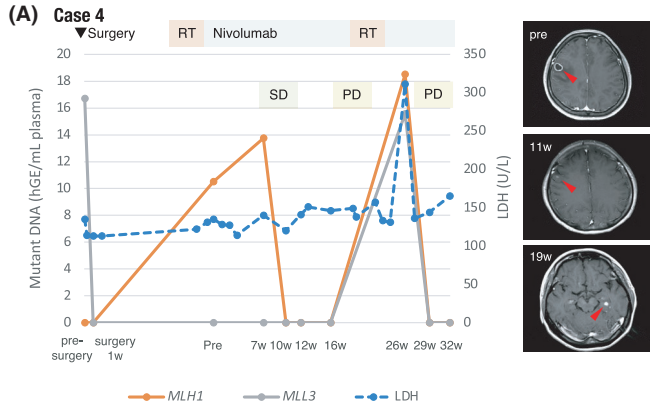
mutations derived from different tumor clones with altered reactivity to therapy.

We sequenced tumor DNA from archival tumor tissues from cases 5, 9, 17, 23, and 38 using the same gene panel and sequencing platform for ctDNA analysis (Table S5). None of the somatic mutations identified in case 5 was common between the tumor tissues and plasma DNA samples. Considering that VAFs of mutations detected in the tumor tissue were low (0.006-0.025), they were

presumably subclonal mutations and could not be detected in the plasma. Tumor tissue and plasma DNA from case 9 showed identical mutations in *BRAF*, suggesting mutant *BRAF* to be the driver of melanoma progression that was derived from melanoma. Therefore, the BRAF/MEK inhibitor, vemurafenib, was administered before the immune checkpoint blockade therapy in case 9. After 3 mo with vemurafenib, progression of the disease was observed using computed tomography. Moreover, *BRAF* mutations were detected in the tumor tissue from case 17. However, this mutation was not detected in the plasma DNA. Instead, we identified a mutant *MET* in the plasma before and after surgery. As mutant *MET* was not detected in the tumor samples used for sequencing, ctDNA derived from different subclones harboring *MET* amplification might be dominant in the plasma (Figure 2F). Targeted sequencing analysis did not detect somatic mutations in the plasma DNA from cases 23 and 38.

The data from longitudinal targeted sequencing of ctDNA showed the importance of liquid biopsy in determining clonal changes in patients with melanoma undergoing therapy. Several mutations that were undetectable before treatment were identified in plasma DNA collected at the time points corresponding to acute exacerbation with massive ascites in case 12 (Figure 2D). This indicates the expansive evolution of tumor clones during immunotherapy.

To further understand the changes in the ctDNA mutational profiles of case 12, we performed WES using plasma DNA. Plasma DNA samples obtained before therapy (Pre), 12 wk (12w), and 16 wk (16w) after initiation of therapy were subjected to WES analysis. We obtained sequencing reads for Pre, 12w, and 16w plasma DNA samples, with mean unique sequencing coverages of 286.3×, 446.3×, and 531.3×, respectively. Somatic mutations in the plasma DNA were initially detected with a threshold of VAF > 0.006, and the numbers of reads supporting a mutation for plasma DNA were at least 8. Using these criteria, we identified 226, 391, and 746 somatic mutations (SNVs and short indel) in the Pre, 12w, and 16w plasma DNA samples, respectively (Table S6). We then modified the threshold of the number of mutant reads to normalize the detectability of somatic mutations in plasma DNA by adjusting for sequencing coverage to 8, 12.47, and 14.84 for Pre, 12w, and 16w plasma DNA, respectively. We detected 226, 112, and 220 somatic mutations using the Pre, 12w, and 16w plasma samples, respectively.

We detected 78 identical mutations at 2 or more time points. Figure 3A shows the changes in VAF of the identical mutations. Among these, only 3 mutations were detected at 3 time points. Thirteen mutations detected in the Pre and 12w plasma samples were undetectable in the plasma collected at 16w, suggesting the reduction of subclones harboring these mutations during therapy. VAFs of 59 mutations detected in the plasma before therapy were undetectable at 12w before increasing at 16w. Moreover, 3 mutations that were not detected in the pretreated plasma were found in the 12w and 16w samples, suggesting that those mutations were derived from expanding subclones during cancer progression.

Figure 3B shows the commonalities of the somatic mutations detected in the plasma. Although 78 mutations were detected across
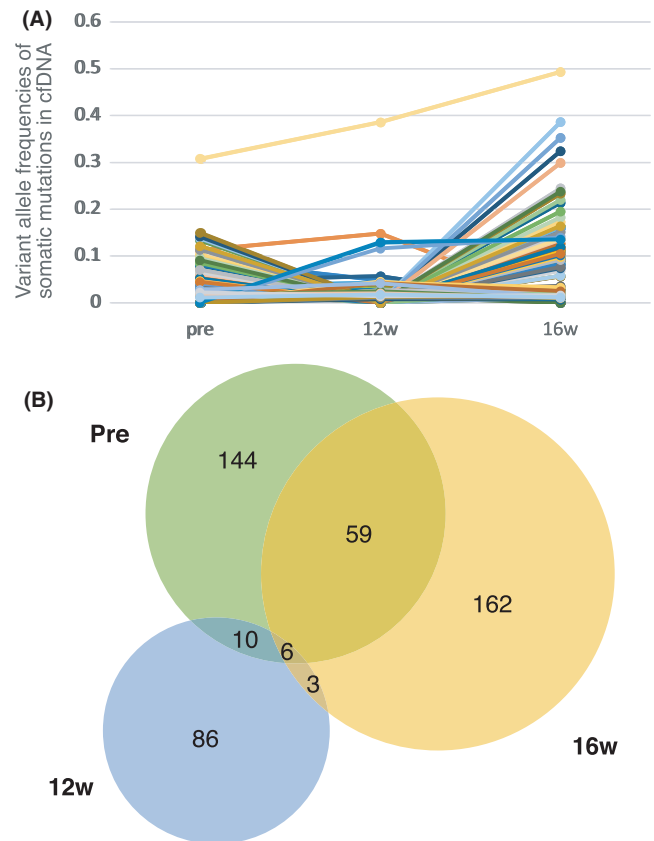

FIGURE 3 Somatic mutations detected in plasma DNA from case 12 using WES. A, Chronological changes in variant allele frequencies of mutations detected in plasma DNA using WES. In total, 78 somatic mutations identified at multiple time points are shown in the plot. B, Venn diagram of somatic mutations detected in plasma DNA using WES. Somatic mutations detected in samples collected before therapy (Pre) are in green, at week 12 (12w) are in blue, and at week 16 (16w) are in yellow. WES, whole-exome sequencing

2 or 3 time points, the vast majority of mutations were detected at a single time point. As much as 162 mutations detected in the 16w plasma DNA could not be detected in the earlier plasma DNA samples. This implies the evolution of multiple subclones after 12w and before acute exacerbation (eg, massive ascites) in this patient. Therefore, the changes in the composition of cancer subclones during therapy might reflect a patient's clinical disease status.

4 | DISCUSSION

In this study, we investigated the mutational profiles of ctDNA and its changes during immune checkpoint blockade therapy in Japanese patients with malignant melanoma. Retrospective WES analysis confirmed the presence of ctDNA with somatic mutations, including subclonal mutations in the pretreatment plasma. *BRAF* and *NRAS* are frequently mutated in melanoma; therefore, hotspot mutations in these genes have been used as ctDNA biomarkers in the Western population.[13,15-17] However, Asian populations have lower rates

of mutation in *BRAF* or *NRAS* than do Caucasian populations.[29-31] The majority of mucosal or uveal melanomas do not have mutant *BRAF*.[32-35] In our 21 plasma DNA samples subjected to WES, we observed that 33% of the samples had mutant *BRAF* or *NRAS*. Therefore, ctDNA analysis of these hotspot mutations might be insufficient for Japanese melanoma cases.

Prospective longitudinal analysis of plasma DNA in immune checkpoint inhibitor-treated melanoma patients showed that the amounts of plasma DNA dynamically changed based on treatment and patient status. Plasma DNA levels are regulated by various physiological conditions, including injury and inflammation. Elevation of plasma DNA levels after surgery was observed in cases 4 and 17. Cases 8, 16, and 18 showed transient increases in the amounts of plasma DNA 6-10 wk after immunotherapy initiation. Immune responses associated with immune checkpoint blockade, such as pseudo-progression or immune-related adverse events, are observed within 12 and 10 wk of therapy initiation, respectively.[36,37] The activation of immune responses by immune checkpoint inhibitors affects the total amounts of plasma DNA.

Targeted deep sequencing analysis of plasma DNA showed dynamic changes in mutant ctDNA levels during therapy, demonstrating the correlation between ctDNA and response to therapy. However, discrimination between pseudo- and true progression has been challenging in cancer immunotherapy. Case 18 experienced pseudo-progression. Interestingly, ctDNA levels decreased within 12 wk of nivolumab initiation despite a slight increase in tumor size. Although ctDNA levels increased after pseudo-progression (15 wk), mutant ctDNA was undetectable at the next time point, and the target lesion gradually decreased, thereby resulting in PR and suggesting the utility of ctDNA analysis in differentiating between pseudo- and true progression. The transient increase in ctDNA in case 18 could be because of damaged cancer cells by the cytotoxicity of immune cells. Case 8 also showed transient increases in ctDNA after radiotherapy. As the effects of radiation are observed several months after irradiation, the transient elevation of ctDNA could be due to the radiotherapy-induced death of tumor cells. The elevation of ctDNA levels is not always associated with disease progression in patients undergoing immunotherapy.

Another challenge in cancer therapy is characterizing refractory clones to therapy. Liquid biopsy can detect mutations derived from different tumor clones from multiple lesions with different reactivities to therapy. ctDNA analysis could be valuable in characterizing responsive and refractory clones. In case 8, durable SD was documented throughout follow-up. While *MSH3* mutations were constantly detected in ctDNA, mutations in *ARID1B* transiently appeared 13-17 wk after radiotherapy. As no other malignancy was documented in this case, these mutations might be derived from different tumor cell clones. Notably, suppression of ARID1B impairs DNA repair and sensitizes cells to ionizing radiation.[38]

Interestingly, WES of plasma DNA from case 12 revealed a dramatic change in mutational profiles of ctDNA during immunotherapy. While a variety of somatic mutations in ctDNA increased with progressing disease, WES showed an abrupt increase in somatic mutations exclusively detected in plasma at a single time point. In accordance with the reported changes in mutational profiles in tumor tissues during therapy,[11,12] our results suggest a drastic alteration in the composition of tumor subclones in a patient during immunotherapy.

However, there are some limitations to this study. First, the patient cohort was limited, and a larger cohort should be studied to understand the utility of ctDNA analysis in monitoring cancer during immunotherapy. Second, the 74-gene panel designed for targeted deep sequencing might be insufficient to assess chronological changes in ctDNA in some patients. No identical mutation was detected at different time points in 6 of 14 patients in targeted sequencing of plasma DNA, suggesting the presence of clonal mutations outside the target region of our gene panel. A more comprehensive analysis, such as WES, may help determine the mutational profiles of ctDNA in a wide range of patients undergoing immune checkpoint blockade therapy.

In conclusion, we showed that longitudinal ctDNA analysis could potentially monitor response to therapy, including pseudo-progression, and help understand clonal evolution during therapy in melanoma patients. The timely assessment of ctDNA mutational profiles might help devise treatment strategies.

DISCLOSURE

The authors declare no conflict of interest.

ORCID

Satoshi Shiba 🆔 https://orcid.org/0000-0001-5159-5719
Kenjiro Namikawa 🆔 https://orcid.org/0000-0003-2763-7346
Naoya Yamazaki 🆔 https://orcid.org/0000-0002-9638-0428
Tatsuhiro Shibata 🆔 https://orcid.org/0000-0002-0477-210X
Shinichi Yachida 🆔 https://orcid.org/0000-0001-5507-4566

REFERENCES

1. Topalian SL, Hodi FS, Brahmer JR, et al. Safety, activity, and immune correlates of anti-PD-1 antibody in cancer. *N Engl J Med.* 2012;366(26):2443-2454.

2. Robert C, Long GV, Brady B, et al. Nivolumab in previously untreated melanoma without BRAF mutation. *N Engl J Med*. 2015;372(4):320-330.

3. Hodi FS, O'Day SJ, McDermott DF, et al. Improved survival with ipilimumab in patients with metastatic melanoma. *N Engl J Med*. 2010;363(8):711-723.

4. Brahmer J, Reckamp KL, Baas P, et al. Nivolumab versus docetaxel in advanced squamous-cell non-small-cell lung cancer. *N Engl J Med*. 2015;373(2):123-135.

5. Borghaei H, Paz-Ares L, Horn L, et al. Nivolumab versus docetaxel in advanced nonsquamous non-small-cell lung cancer. *N Engl J Med*. 2015;373(17):1627-1639.

6. Reck M, Rodriguez-Abreu D, Robinson AG, et al. Pembrolizumab versus chemotherapy for PD-L1-positive non-small-cell lung cancer. *N Engl J Med*. 2016;375(19):1823-1833.

7. Motzer RJ, Escudier B, McDermott DF, et al. Nivolumab versus everolimus in advanced renal-cell carcinoma. *N Engl J Med*. 2015;373(19):1803-1813.

8. Grassadonia A, Sperduti I, Vici P, et al. Effect of gender on the outcome of patients receiving immune checkpoint inhibitors for advanced cancer: a systematic review and meta-analysis of phase III randomized clinical trials. *J Clin Med*. 2018;7(12):542.

9. Pogrebniak KL, Curtis C. Harnessing tumor evolution to circumvent resistance. *Trends Genet*. 2018;34(8):639-651.

10. Hachey SJ, Boiko AD. Therapeutic implications of melanoma heterogeneity. *Exp Dermatol*. 2016;25(7):497-500.

11. Riaz N, Havel JJ, Makarov V, et al. Tumor and microenvironment evolution during immunotherapy with nivolumab. *Cell*. 2017;171(4):934-49 e16.

12. Anagnostou V, Smith KN, Forde PM, et al. Evolution of neoantigen landscape during immune checkpoint blockade in non-small cell lung cancer. *Cancer Discov*. 2017;7(3):264-276.

13. Calbet-Llopart N, Potrony M, Tell-Marti G, et al. Detection of cell-free circulating BRAF(V) (600E) by droplet digital polymerase chain reaction in patients with and without melanoma under dermatological surveillance. *Br J Dermatol*. 2020;182(2):382-389.

14. Lipson EJ, Velculescu VE, Pritchard TS, et al. Circulating tumor DNA analysis as a real-time method for monitoring tumor burden in melanoma patients undergoing treatment with immune checkpoint blockade. *J Immunother Cancer*. 2014;2(1):42.

15. Tsao SC, Weiss J, Hudson C, et al. Monitoring response to therapy in melanoma by quantifying circulating tumour DNA with droplet digital PCR for BRAF and NRAS mutations. *Sci Rep*. 2015;5:11198.

16. Xi L, Pham TH, Payabyab EC, et al. Circulating tumor DNA as an early indicator of response to T-cell transfer immunotherapy in metastatic melanoma. *Clin Cancer Res*. 2016;22(22):5480-5486.

17. Lee JH, Long GV, Boyd S, et al. Circulating tumour DNA predicts response to anti-PD1 antibodies in metastatic melanoma. *Ann Oncol*. 2017;28(5):1130-1136.

18. Gremel G, Lee RJ, Girotti MR, et al. Distinct subclonal tumour responses to therapy revealed by circulating cell-free DNA. *Ann Oncol*. 2016;27(10):1959-1965.

19. Cutts A, Venn O, Dilthey A, et al. Characterisation of the changing genomic landscape of metastatic melanoma using cell free DNA. *NPJ Genom Med*. 2017;2:25.

20. Rago C, Huso DL, Diehl F, et al. Serial assessment of human tumor burdens in mice by the analysis of circulating DNA. *Cancer Res*. 2007;67(19):9364-9370.

21. Takai E, Totoki Y, Nakamura H, et al. Clinical utility of circulating tumor DNA for molecular assessment in pancreatic cancer. *Sci Rep*. 2015;5:18425.

22. Hodis E, Watson IR, Kryukov GV, et al. A landscape of driver mutations in melanoma. *Cell*. 2012;150(2):251-263.

23. Rizvi NA, Hellmann MD, Snyder A, et al. Mutational landscape determines sensitivity to PD-1 blockade in non-small cell lung cancer. *Science*. 2015;348(6230):124-128.

24. Zaretsky JM, Garcia-Diaz A, Shin DS, et al. Mutations associated with acquired resistance to PD-1 blockade in melanoma. *N Engl J Med*. 2016;375(9):819-829.

25. Shi H, Hugo W, Kong X, et al. Acquired resistance and clonal evolution in melanoma during BRAF inhibitor therapy. *Cancer Discov*. 2014;4(1):80-93.

26. Jones S, Anagnostou V, Lytle K, et al. Personalized genomic analyses for cancer mutation discovery and interpretation. *Sci Transl Med*. 2015;7(283):283ra53.

27. Li H, Durbin R. Fast and accurate long-read alignment with Burrows-Wheeler transform. *Bioinformatics*. 2010;26(5):589-595.

28. Li H, Handsaker B, Wysoker A, et al. The Sequence Alignment/Map format and SAMtools. *Bioinformatics*. 2009;25(16):2078-2079.

29. Kim SY, Kim SN, Hahn HJ, et al. Metaanalysis of BRAF mutations and clinicopathologic characteristics in primary melanoma. *J Am Acad Dermatol*. 2015;72(6):1036-46 e2.

30. Sakaizawa K, Ashida A, Uchiyama A, et al. Clinical characteristics associated with BRAF, NRAS and KIT mutations in Japanese melanoma patients. *J Dermatol Sci*. 2015;80(1):33-37.

31. Kaji T, Yamasaki O, Takata M, et al. Comparative study on driver mutations in primary and metastatic melanomas at a single Japanese institute: a clue for intra- and inter-tumor heterogeneity. *J Dermatol Sci*. 2017;85(1):51-57.

32. Zhou R, Shi C, Tao W, et al. Analysis of mucosal melanoma whole-genome landscapes reveals clinically relevant genomic aberrations. *Clin Cancer Res*. 2019;25(12):3548-3560.

33. Spencer KR, Mehnert JM. Mucosal melanoma: epidemiology, biology and treatment. *Cancer Treat Res*. 2016;167:295-320.

34. Saldanha G, Purnell D, Fletcher A, et al. High BRAF mutation frequency does not characterize all melanocytic tumor types. *Int J Cancer*. 2004;111(5):705-710.

35. Zuidervaart W, van Nieuwpoort F, Stark M, et al. Activation of the MAPK pathway is a common event in uveal melanomas although it rarely occurs through mutation of BRAF or RAS. *Br J Cancer*. 2005;92(11):2032-2038.

36. Wolchok JD, Hoos A, O'Day S, et al. Guidelines for the evaluation of immune therapy activity in solid tumors: immune-related response criteria. *Clin Cancer Res*. 2009;15(23):7412-7420.

37. Weinstein A, Gordon RA, Kasler MK, et al. Understanding and managing immune-related adverse events associated with immune checkpoint inhibitors in patients with advanced melanoma. *J Adv Pract Oncol*. 2017;8(1):58-72.

38. Watanabe R, Ui A, Kanno S, et al. SWI/SNF factors required for cellular resistance to DNA damage include ARID1A and ARID1B and show interdependent protein stability. *Cancer Res*. 2014;74(9):2465-2475.

SUPPORTING INFORMATION

Additional supporting information may be found in the online version of the article at the publisher's website.